A Hybrid DWT-SVD Based Adaptive Image Watermarking Scheme

Sachin Gaur *, Navneet Tripathi, and Jyoti Pandey

Department of Computer Science and Engineering, B. T. Kumaon Institute of Technology Dwarahat, Uttarakhand Technical University Dehradun, India; Email: tnavneet751@gmail.com (N.T.), jyotipandey7531@gmail.com (J.P.)
*Correspondence: ersgaur1234@gmail.com (S.G.)

***Abstract*—In the digital age, protecting the ownership and data veracity of digital documents is a major challenge. To address the issues concerning copyright protection and data verification of digital media, digital watermarking has emerged as a solution. In this paper, we aspire to make a modest contribution to this emerging and exciting field by presenting our proposed adaptive hybrid image watermarking approach that combines Discrete Wavelet Transform (DWT) and Singular Value Decomposition (SVD). Our method involves applying DWT to both the host image and watermark, followed by singular decomposition using SVD on the Low-Low (LL) component of both images. Now modify the singular values of the host image by the singular values of the watermark, and then inverse SVD is applied, followed by inverse DWT, to obtain the watermarked image. After that, the reverse process is applied to obtain the watermark image. Finally, we evaluate our approach's performance by measuring the Peak Signal-to-Noise Ratio (PSNR) between the original and watermarked image as well as the Normalized Cross-Correlation (NCC) between the original and extracted watermark. Simulation results indicate that the proposed method is rich in terms of robustness, imperceptibility and capacity than the previously presented schemes.**

***Keywords*—digital image watermarking, discrete wavelet transform, singular value decomposition, particle swarm optimization, Normalized Cross-Correlation (NCC) and Peak Signal-to-Noise Ratio (PSNR)**

I. Introduction

In contemporary times, we are experiencing an era dominated by computers, characterized by the advent of the Digital Revolution, which renders us less reliant on manually operated machinery. The current trend is inclined towards automation, and nearly all physical entities have a corresponding virtual digital counterpart. The speedy progression in the realm of information technology and the Internet has expedited this process. On a global scale, the Internet facilitates the generation, consumption, and transmission of an immense volume of digital media every second. The massive production and utilization of digital media gives rise to issues related to safeguarding copyright and verifying data authenticity. The domain of digital watermarking is a promising and dynamic field that focuses on addressing these issues [1, 2]. The primary objective of this research paper is to explore the utility of digital image watermarking as a potential solution to mitigate the concerns surrounding copyright violation and data verification [3]. Digital watermarking is the mechanism of adding a visible or invisible identifier to a digital medium, be it an image, audio, video file, or document, to protect it from unauthorized use and distribution. The embedded watermark, depending on the specific use case, must possess qualities of imperceptibility and robustness to withstand potential external attacks [4].

The concept of imperceptibility pertains to the extent to which a watermark can be detected or discerned by the human eye, while robustness refers to the ability of the watermark to withstand diverse forms of attack. The imperceptibility and robustness characteristics are determined using the Peak Signal-to-Noise Ratio (PSNR) analysis conducted on the original and watermarked images (for imperceptibility analysis) and the Normalized Cross-Correlation (NCC) assessment performed on the original and extracted watermark (for robustness analysis). The utilization of digital watermarking is widespread across various domains that encompass the creation and dissemination of electronic records, including but not limited to military operations, medical research, and the entertainment industry [5, 6].

The classification of digital image watermarking techniques is primarily based on two categories, namely, spatial domain and frequency domain. The spatial domain views an image as a combination of pixels, and these techniques directly work on manipulating the intensity values of the pixels of the original image [7]. Spatial-domain methods are relatively less intricate and time-efficient, but they exhibit limitations in terms of robustness. Spatial domain methods for digital image watermarking encompass various established techniques such as Least Significant Bit (LSB) imitation, Pixel Value Differencing (PVD), Exploiting Modification Direction (EMD), and Modulus Function (MF) [8, 9]. The technique of LSB steganography involves concealing confidential data within the pixel values of the host image [10].

Frequency domain methods involve the incorporation of watermarks onto the transformed image coefficients

Manuscript received June 14, 2023; revised July 6, 2023; accepted September 7, 2023.

obtained through the utilization of transformation functions such as DFT, DCT, DWT, and others [11–14]. Despite the complex and computationally demanding nature of frequency domain techniques, they demonstrate excellent performance metrics in terms of high imperceptibility and robustness. Our research presents a novel adaptive watermarking method that combines Discrete Wavelet Transform (DWT) and Singular Value Decomposition (SVD) in a hybrid approach. The objective of the proposed hybrid approach is to combine the strengths of DWT and SVD to boost the effectiveness of watermarking. Specifically, DWT provides advantages such as spatial and frequency localization, while SVD improves the watermark's resilience against various types of attacks. The necessity for reliable and undetectable watermarking methods to safeguard digital multimedia information against unauthorised use, manipulation, and copyright infringement served as the motivation behind the development of a hybrid DWT-SVD-based adaptive image watermarking strategy. Digital watermarking is the technique of incorporating a hidden watermark that can be reliably recovered by authorised parties but is difficult for the human eye to notice into multimedia output (such as images, audio, or video). The contribution of the proposed work is to enhance robustness, imperceptibility, security, and capacity.

It is briefly explained how the paper was reorganized to be systematized as in the Section II literature survey, SVD, DWT, and PSO. Section III discusses the embedding and removal processes. The results and a comparison of our technique are presented in Section IV, and the paper's conclusion is discussed in Section V.

II. Literature Survey

This section will explore previous studies carried out in the field of digital image watermarking, which have served as a source of inspiration for our current research proposal. Gunjal *et al.* [15] presented a comprehensive introduction to digital image watermarking, and a thorough comparison was conducted between spatial domain techniques and transform domain methods. This paper offers a concise summary of various spatial domain and transform domain techniques, including their general implementation and mathematical formulations, as well as their strengths and limitations. After conducting their research, the authors suggest the utilization of DWT-based techniques to attain robustness in digital image watermarking.

Deb *et al.* [16] proposed a robust technique for copyright protection of digital images, combining DWT and DCT. It leverages the spatial localization and scalability of DWT as well as the compression benefits of DCT-based watermarking. Experimental outcomes show superior image aspects and robustness versus various attacks. Sahu *et al.* [17] presented an enhanced image steganographic technique that improves capacity and PSNR using modified LSB substitution and matching principles. The technique includes three variations, each utilizing a 2-pixel block for data embedding. Experimental results demonstrate superior performance compared to existing methods. Rao *et al.* [18] proposed a PSO-based digital image watermarking scheme using DWT, DCT, and SVD. The method decomposes the original image into high-frequency sub-bands using DWT and DCT. SVD is applied to these sub-bands to obtain singular values. PSO is used to find optimal embedding parameters. The scheme's effectiveness is evaluated using PSNR, NC coefficient, and BER.

Lin *et al.* [19] introduced a DCT-based image watermarking technique that addresses the challenge of maintaining image quality while enhancing robustness against JPEG compression. They proposed a methodology that adjusts DCT low-frequency coefficients using remainders, achieving near-complete retrieval of embedded watermarks from highly compressed JPEG images in simulations. Yasmeen *et al.* [20] introduced an enhanced hybrid approach that combines DWT and SVD to improve the resilience and safeguarding of digital data. The methodology involves multiple levels of operations using DWT and SVD for embedding and extracting features. The proposed method is validated against various attacks, distinguishing it from existing schemes. It has proven to be an effective system for grayscale and color images.

Thakkar *et al.* [21] proposed a digital image watermarking technique that employs PSO and block-SVD. The methodology partitions the cover image into blocks, extracts singular values through SVD, and determines optimal embedding parameters using PSO. The technique's effectiveness is assessed using metrics like PSNR and NC coefficient, and its resilience against various attacks is examined.

Zear *et al.* [22] proposed a watermarking algorithm for healthcare applications using DWT, DCT, and SVD. The algorithm enhances watermark robustness through noise reduction using BPNN and improves security via the Arnold transform. Experimental results demonstrate the algorithm's superiority and its potential for preventing patient identity theft in healthcare settings. Kumar *et al.* [23] proposed a watermarking approach that utilizes DWT and PSO to identify high-energy coefficient watermark bits and subsequently embed the watermark in the cover image. The scheme's efficacy was evaluated for robustness and imperceptibility against different attacks, demonstrating favourable results.

Liu *et al.* [24] proposed a secure non-blind watermarking technique using DWT, SVD, and RSA encryption. The scheme outperformed alternative methods in terms of CPU running time, PSNR, and NCC metrics. Wu *et al.* [25] introduced a novel image watermarking technique using LSB steganography. Their method divides the image into groups of three pixels, allowing the embedding of three bits of confidential information. The technique outperforms previous LSB-based algorithms, as confirmed by empirical evaluation.

Kuppusamy *et al.* [26] introduced an optimized image watermarking method using PSO. The technique's embedding strength was optimized through PSO, and its robustness against different attacks was evaluated. Empirical results show high resilience against various attacks. Gorai *et al.* [27] proposed a PSO-based method for

enhancing grey-level images. By optimizing the parameters of a nonlinear mapping function using PSO, they improved image contrast. The approach was evaluated using multiple benchmark images, demonstrating significant enhancement compared to existing methods. Ghazy *et al.* [28] introduced an efficient image watermarking approach using the block-by-block SVD technique. The method segments the source image into blocks and inserts the watermark within the Singular Values (SVs) of each block individually. This technique significantly enhances the watermark's resilience against external attacks.

Kang *et al.* [29] proposed an innovative blind image watermarking scheme using a combination of DCT, SVD, least-square curve fitting, and a logistic chaotic map in the DWT domain. The scheme outperforms existing methods in perceptual quality and resilience against signal processing and geometric attacks. Hu *et al.* [30] proposed a robust and efficient image watermarking algorithm using 1D Empirical Mode Decomposition (EMD) and dimensional reduction with the Hilbert curve. The algorithm reduces computational expenses and exhibits superior resilience against external attacks compared to other state-of-the-art schemes.

Agoyi *et al.* [31] introduced a novel watermarking scheme that combines the DWT with the Chirp Z-Transform (CZT) and the SVD. Experimental results demonstrate that the CZT-DWT-SVD approach offers enhanced imperceptibility and robustness against various attacks and signal processing operations. Wand and Zhao [32] introduced an adaptive image watermarking method that combines SVD with the Wang-Landau (WL) sampling technique. The method was validated against image processing attacks, demonstrating a balance between robustness and invisibility.

Das *et al.* [33] introduced an innovative blind watermarking algorithm in the DCT domain, leveraging the correlation between adjacent DCT coefficients in the same position. The scheme exhibits exceptional robustness against JPEG compression and effectively extracts high-quality watermarks even under common image processing operations. Makbol *et al.* [34] proposed a reliable SVD-based watermarking approach by using Integer Wavelet Transform (IWT) with ant colony optimization, in this scheme, the U metric of the grey scale watermarked is embedded into the singular values of the LL subband image to remove the false positive problem and also improve robustness and imperceptibility.

Roy *et al.* [35] proposed a RDWT-DCT-based image watermarking scheme with the Arnold scramble method to improve the robustness and watermark image. Ali *et al.* [36] presented a novel watermarking scheme in which the invariant blocks that are used for watermarking are found and the SVD is applied to that block that has the largest singular value, and then the principal components of the watermark image are inserted into these blocks to improve the result for geometrical attack. Ansari *et al.* [37] proposed a DWT-SVD-based multipurpose image watermarking algorithm with Artificial Bee Colony (ABC), in which the DWT-transformed host image is modified to modify the principal components of robust watermark insertion in the last two LSB and remove the false positive problem. They also proved the decent capacity as well as robustness and imperceptibility. Radha *et al.* [38] proposed a Deep Belief Network (DBN) and Bear Smell Search Algorithm (BSSA)-based DWT-SVD hybrid watermarking method, in which for embedding the watermark by using hybrid transform domain is performed and for extraction Back Propagation Neural Network (BPNN) is used and then achieved good imperceptibility and robustness from the previous presented scheme.

The necessity for reliable and undetectable watermarking methods to safeguard digital multimedia information against unauthorised use, manipulation, and copyright infringement served as the motivation behind the development of a hybrid DWT-SVD-based adaptive image watermarking strategy. Digital watermarking is the technique of incorporating a hidden watermark that can be reliably recovered by authorised parties but is difficult for the human eye to notice into multimedia output (such as images, audio, or video). The contribution of the proposed work is to enhance robustness, imperceptibility, security, and capacity. This division is dedicated to providing concise descriptions of the key ideas utilized in the presented scheme, which include DWT, SVD transforms, and Particle Swarm Optimization (PSO). Those who are interested in obtaining a more detailed understanding may refer to the corresponding studies [39–45].

A. Discrete Wavelet Transform (DWT)

The Discrete Wavelet Transform (DWT) is extensively used for digital image watermarking. The process entails converting the image into its frequency domain using the wavelet transform, which decomposes the image into different frequency components, revealing the time-frequency representation of the original signal. Wavelets are unique functions that serve as the fundamental building blocks for signal representation, similar to sines and cosines in Fourier analysis. Unlike the traditional Fourier transform, which provides a global frequency analysis, the DWT captures both frequency and time information at different resolutions. For 2-D images, the DWT application involves executing 2-D filters in each dimension. These filters segment the input image into four non-overlapping sub-bands, namely LL, LH, HL, and HH, each consisting of multi-resolution coefficients. Among these sub-bands, LL and other sub-bands (LH, HL, and HH) mean the fine-scale DWT coefficients. Typically, the majority of the image energy is concentrated in the lower transform sub-bands, i.e., LL, so embedding the watermark in these sub-bands significantly degrades the image quality. However, embedding a watermark in the low-transform sub-bands can lead to a significant increase in robustness. On the other hand, the high-frequency sub-bands, i.e., HH, contain the image's edges and textures, which are not usually sensitive to changes as perceived by the human eye. This enables watermark embedding without being noticeable to the human eye. Many DWT-based watermarking algorithms compromise by embedding the watermark in the middle frequency sub-bands, i.e., LH and HL, where they can achieve acceptable performance in terms of

imperceptibility and robustness [40–43]. The DWT technique presents numerous benefits, such as enhanced security, robustness, and imperceptibility, making it particularly useful for applications that demand high levels of security and robustness, such as digital forensics, copyright protection, and image authentication. The DWT of a signal is defined by the following equations:

$$W_\phi(j_o,\ k) = \frac{1}{\sqrt{M}} \sum_x f(x) \phi_{j_o,\ k}(x) \quad (1)$$

$$W_\psi(j,\ k) = \frac{1}{\sqrt{M}} \sum_k f(x) \psi_{j,\ k}(x) \quad (2)$$

For, $j \geq j_o$ and the Inverse DWT (IDWT) is defined as:

$$f(x) = \frac{1}{\sqrt{M}} \sum_k W_\phi(j_o,\ k) \phi_{j_o,k}(x) \ + \frac{1}{\sqrt{M}} \sum_{j=j_o}^{\infty} \sum_k W_\psi(j,\ k) \psi_{j,k}(x) \quad (3)$$

where: $f(x),\ \phi_{j_o,k}(x)\ and\ \psi_{j,k}(x)$ are functions of the discrete variable x = 0, 1, 2, M−1. Fig. 1 shows the 1-level DWT transform on Lena image, here low transform component shows the most content of the host image Lena and high transform component shows the edge and texture characteristics of the original image.

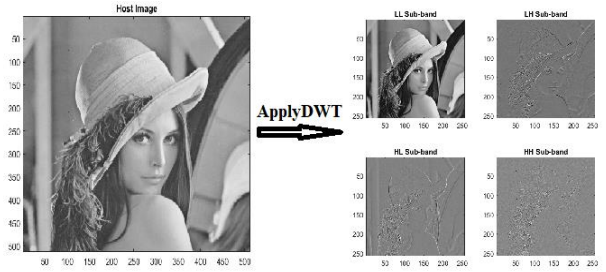

Figure 1. DWT Decomposition Image of Lena (512×512) in to four sub band (LL, LH, HL, HH).

B. Singular Value Decomposition (SVD)

Singular Value Decomposition is a linear algebra transform used to factorize or decompose a real or complex matrix into its three constituents: a left singular matrix, a diagonal matrix of its singular values, and a right singular matrix. The left singular matrix is an orthogonal matrix, which represents the relationship between the columns of the original matrix. The diagonal matrix S contains the singular values of the original matrix, arranged in descending order along its diagonal. The columns form an orthonormal basis for the column space of the original matrix. These singular values represent the relative importance of the different patterns or features in the original matrix. The larger the singular value, the more important the corresponding pattern or feature is. The right singular matrix is also an orthogonal matrix, which represents the relationship between the rows of the original matrix. The columns form an orthonormal space for the row space of the original matrix.

$$A \rightarrow USV^T \quad (4)$$

The process of reconstructing the original matrix $'A'$ is achieved by multiplying the matrices $U,\ V$ and S. This procedure is commonly referred to as the inverse SVD.

$$A \leftarrow USV^T \quad (5)$$

Singular Value Decomposition (SVD) can be interpreted as a matrix transformation procedure [44]. Overall, the resultant matrices of SVD tell us about the relationships and patterns within the original matrix, allowing us to analyze and modify data in various ways. SVD is a powerful mathematical tool in fields like image processing, data analysis, and machine learning. In image processing, SVD decomposition is used for various purposes, like image compression by selecting only the significant singular values and disregarding the rest, image enhancement by modifying the singular values of the image, or watermarking.

Singular value decomposition is a widely used technique in digital image watermarking that decomposes an image into its constituent parts, including its singular values. In digital image watermarking, by modifying the singular values in a way that is undetectable by the human eye, a watermark can be inserted into the image, which can be later extracted from the watermarked image. This technique is very efficient in ensuring the authenticity and integrity of digital images. Hence, SVD is used in fields like copyright protection and digital forensics. One of the appealing mathematical aspects of SVD is that minor modifications in singular values have no effect on how the input image appears to the eye. This property drives the watermark embedding process to increase transparency and resilience [45].

C. Particle Swarm Optimization (PSO)

Particle Swarm Optimization (PSO) is a powerful technique that is based on the social behaviour of individuals in nature, such as a group of birds or a group of fish. The idea behind this is that groups of individuals, called particles, move freely through the search space to find the best possible solution to a particular problem. The PSO algorithm is very flexible and can be applied to many types of problems; it does not require knowledge of the function to be optimized and uses only mathematical operations. Each particle has a position, velocity, and memory that update over time as it moves through the search space. One advantage of PSO is that each particle can learn from its personal experience and share that information with other particles [21, 23]. This allows the swarm to explore the search space more efficiently and find better solutions. The PSO algorithm defines each particle as a potential solution to an n-dimensional problem. Each particle's velocity is increased using an equation that takes into account its current velocity, its personal best solution, and its global best position. The particles will update their positions with this new velocity. Each particle's velocity is increased using Eq. (6), and each particle updates its position using Eq. (7).

$$V_{t+1}^r = W \times V_t^r + C_1 \times rand_1 \times (P_t - X_t^r) + C_2 \times rand_2 \times (G_t - X_t^r) \quad (6)$$

$$X_{t+1}^{r} = X_{t}^{r} + V_{t+1}^{r} \quad (7)$$

where,

V_t^r : The velocity of the particle 'r' at time 't'.

W : The inertia mass that regulates how the prior velocity affects the present velocity. It is constant value between 0 and 1

C_1: The cognitive parameter that controls the influence of the personal best position on the recent velocity.

P_t: The personal best position of the particle 'r' at iteration

X_t^r: The current position of particle r at iteration t.

C_2: The social parameter that controls the impact of the global best position on recent velocity.

$rand_1\ and\ rand_2$: Random number generator uniformly between 0 and 1 that controls the stochastic behavior of the algorithm

G_t; The global best position of all particle at iteration *t*.

Eq. (6) calculates the new velocity of the particle by combining its recent velocity, the difference between its recent position and the personal best position, and the difference between its recent position and the global best position. The cognitive and social perimeters (and)) determine the influence of personal and global best positions, respectively, on the particle's velocity. The random numbers add stochastic to the program. Eq. (7) updates the position of the particles by adding their new velocity to their current position. This equation moves the particle towards a better position in the search space. These equations are iteratively applied to all particles in the swarm until a termination condition is met, such as reaching the maximum number of iterations or reaching the desired label of convergence. The goal of the PSO algorithm is to find an optimal solution in the problem space by iteratively adjusting the position and velocities of the particles in the swarm.

In order to correctly tune the scale factor with shorter execution times, a block-SVD based watermarking system is integrated with an efficient optimization algorithm, PSO, in this article. For defining the optimization parameters, the PSO algorithm defines swarm size, maximum number of iterations weather to display intermediate result or not. For optimization of fitness function that is a function that takes in a candidate solution (in this case, the scaling factor alpha) and returns a fitness value that qualifies how well solution performs the task at embedding and extracting the watermark. On the basis of PSO fitness function, the fitness function is determined.

To find the ideal scaling factor PSO is applied to find the optimal scaling factor that maximize the fitness function and iteratively updates the particles solution depend on their fitness value.

At the final iteration of the method currently being used, maximum fitness is gained. The following equation gives the mathematical definition of the fitness function.

$$f_{itness} = \max \frac{[Cor(w_o, w^e + Cor(I, I^*]}{2} \quad (8)$$

In Eq. (8), $'cor'$ specifies the normalized correlation coefficient and variables w_o and I signify the watermark and input image w^e and I^* are the extracted watermark and watermarked images [26, 27].

III. Proposed Sheme

The suggested algorithm is a hybrid image watermarking approach based on DWT, SVD, and Particle Swarm Optimization (PSO), in which DWT is applied to both the host image and watermark, followed by singular decomposition using SVD on the Low-Low (LL) component of both images. Now modify the singular values of the input image by the singular values of the watermark, and then inverse SVD is applied, followed by inverse DWT, to obtain the watermarked image. After that, the reverse process is applied to obtain the watermark image. The steps for embedding and extracting watermarks are as follows:

A. Watermark Embedding

Below is a description of the embedding algorithm explained step by step, as shown in Fig. 2:

Step 1: Perform1-level DWT on the host image $'I'$ for decomposing it into four sub-bands.

$$[LL_I, LH_I, HL_I, HH_I] = DWT(I) \quad (9)$$

Similarly to extract four sub-bands from the watermark image W also apply 1-level DWT on It.

$$[LL_W, LH_W, HL_W, HH_W] = DWT(W) \quad (10)$$

Step 2: Decompose low frequency sub-band $'LL_I'$ of the host image into three components using SVD.

$$[U_I, S_I, V_I] = SVD(LL_I) \quad (11)$$

Similarly SVD is applied on the $'LL'$ sub-band of the watermark image to get the three matrices.

$$[U_W, S_W, V_W] = SVD(LL_W) \quad (12)$$

Step 3: Modify singular value component of the input cover image (S_I) by the singular values of the watermark image (S_W) by using the illustrated in Eq. (13).

$$S_I^* = S_I + \alpha \times S_W \quad (13)$$

where α is a scaling factor which is choosing by PSO.

This step involves the incorporation of Particle Swarm Optimization (PSO) to optimize the scaling factor 'α', resulting in enhanced imperceptibility and robustness. The steps involved in optimizing the scaling factor through the use of Particle Swarm Optimization (PSO) are given as:

i. **Defining the optimization parameters:** In this stage, we specify the parameters of the PSO algorithm, including the size of the swarm, the maximum number of iterations, and whether to display intermediate results or not.

ii. **Defining the fitness function for PSO optimization:** The fitness function plays a crucial

role in determining the quality of the solution proposed by the Particle Swarm Optimization (PSO) algorithm. It takes the candidate solution, i.e., the scaling factor alpha, as input and computes a fitness value that reflects the effectiveness of the solution in accomplishing the desired task, i.e., embedding and extracting the watermark. The fitness function is developed by considering the PSO fitness function.

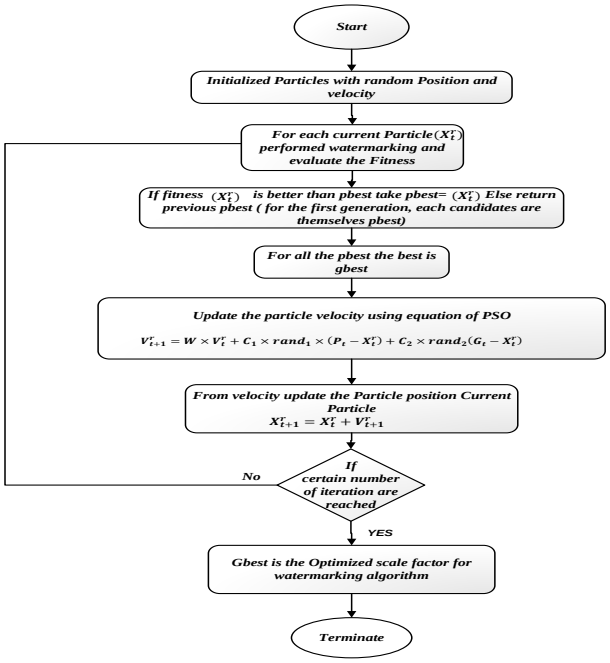

Figure 2. Block diagram of PSO.

iii. **Performing PSO optimization to find the optimal scaling factor:** In this step, the PSO algorithm is utilized to discover the ideal scaling factor alpha that maximizes the fitness function described in Step (ii). The PSO algorithm continually updates the candidate solutions (particles) based on their fitness values and the best solutions found up to that point. The algorithm stops when the maximum number of iterations has been achieved. The block diagram shown in Fig. 3.

Step 4: Now Obtained the modified LL_I^* component by utilizing the orthogonal components (U_I, V_I) with S_I^* of the host image that is inverse SVD is applied.

$$LL_I^* = U_I S_I^* V_I^T \quad (14)$$

where 'T' represent the transpose matrix.

Step 5: Now Perform 1-level inverse DWT on the resulting LL_I^* component obtained from equation 14 to generate the watermarked image W_I.

$$W_I = IDWT(LL_I^* LH_I HL_I HH_I) \quad (15)$$

B. Watermark Extraction

Below is a description of the extraction algorithm explained step by step, as shown in Fig. 4.

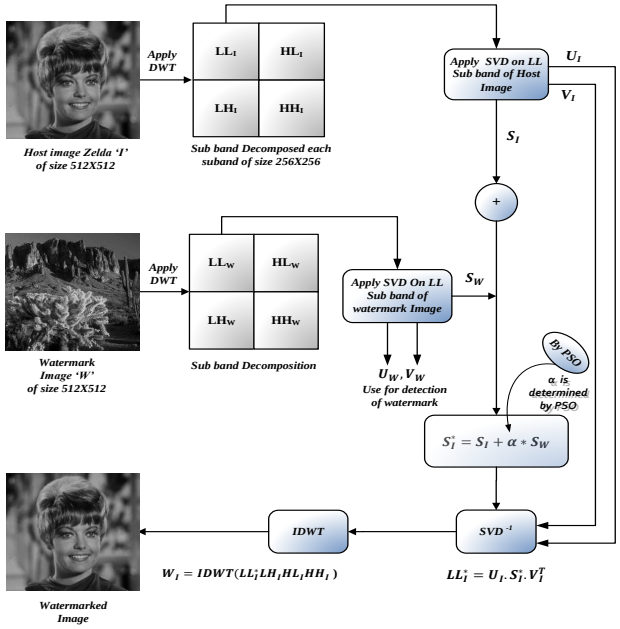

Figure 3. Watermark embedding diagram.

Step 1: Perform1-level DWT on the watermarked image $'W_I'$ to devide it into four sub-bands as.

$$LL_{W_I}, LH_{W_I}, HL_{W_I}, HH_{W_I} = DWT(W_I) \quad (16)$$

Step 2: Perform SVD on the lOW frequency sub-band LL_{W_I} to obtain three components, as illustrated in Eq. (17).

$$U_N . S_N . V_N = SVD\left(LL_{W_I}\right) \quad (17)$$

Step 3: To acquire the singular value component of the extracted watermark $'S_{W_e}'$, subtract the singular value of the original image S_I from the singular value of the received watermarked image S_N divided by the scaling factor α.

$$S_{W_e} = \frac{S_N - S_I}{\alpha} \quad (18)$$

Step 4: Eq. (19) is utilized to recover the Low frequency sub band LL_{W_e} of watermark image by employing the orthogonal component of the watermark image (U_W, V_W) i.e., inverse SVD is applied such as.

$$LL_{W_e} = U_W S_{W_e} V_W^T \quad (19)$$

Step 5: To extract the watermark W_e use the obtained LL_{W_e} component and sub component of the watermark image in the one-level inverse DWT process such as

$$W_e = IDWT\left(LL_{W_e}, LH_W, HL_W, HH_W\right) \quad (20)$$

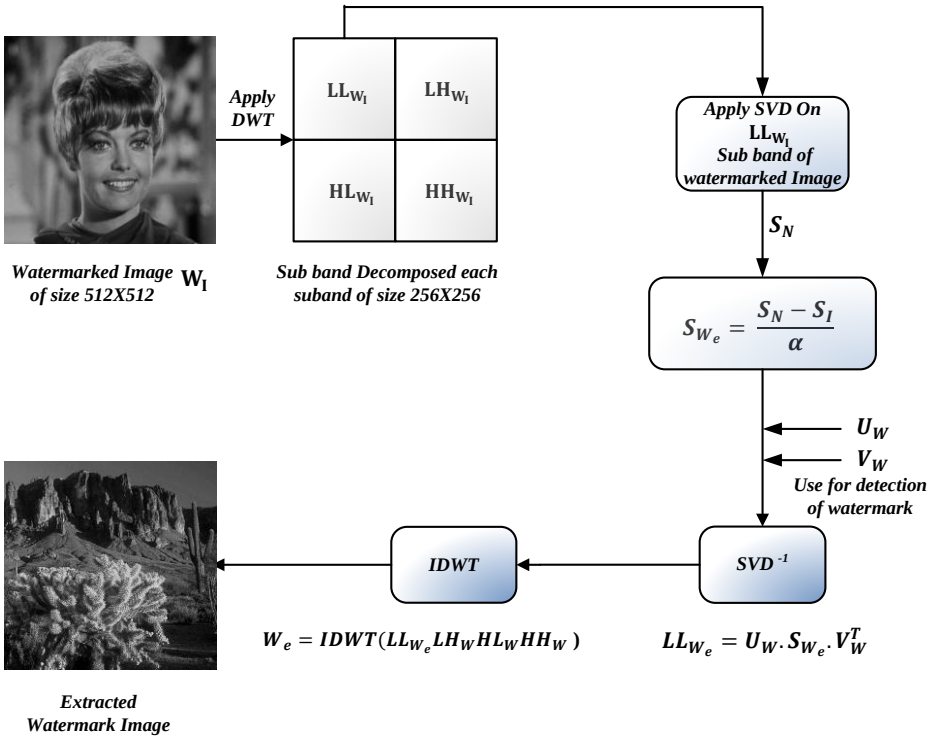

Figure 4. Watermark extraction process.

IV. Experimental Results and Analysis

This section provides a comprehensive analysis, encompassing both qualitative and quantitative assessments, of our proposed image watermarking scheme to determine its effectiveness. We conducted an extensive evaluation to analyze the performance of this scheme in terms of imperceptibility and robustness. To evaluate imperceptibility, there is the Peak-Signal-To-Noise-Ratio (PSNR) metric, which measures the similarity between the original image and the watermarked image. The PSNR is expressed in decibels [31], and in an ideal scenario, its value would be infinite [46]. However, achieving such a value is impossible with a watermarked image. Therefore, a higher PSNR value indicates a better quality of the watermarked image.

The PSNR in decibels (dB) can be calculated using the following Eq. (21):

$$PSNR = 10 \log_{10} \left[\frac{max(x(i,j))^2}{MSE}\right] \quad (21)$$

MSE (Mean square error between host image; *x'* and watermarked image '*y'* can be calculated as

$$MSE = \frac{1}{m \times n} \sum_{i=1}^{M} \sum_{j=1}^{N} [x(i,j) - y(i,j)]^2 \quad (22)$$

Mean Square Error (MSE) is the arithmetic mean of the squared pixel differences among two images. Ideally, the MSE should be zero, but this is not achievable with a watermarked image. As a result, a lower value of MSE indicates better image quality [47]. MSE can be calculated using Eq. (22).

Similarly, to evaluate robustness Normalized Cross-Correlation (NCC) metric is utilized. Normalized Cross-Correlation (NCC) is a commonly used metric in digital image watermarking to evaluate the effectiveness of a watermarking algorithm by measuring the similarity between two images. In an ideal scenario, the NCC value should be 1 [48]. However, in reality, this can only be attained if the watermarked image is not subjected to any form of attack. The NCC value ranges between −1 to 1, where the value of 1 indicates that the two images are a perfect match, 0 indicates no correlation, and −1 indicates a perfect negative correlation. A higher NCC value indicates a greater degree of similarity between the two images. NCC can be calculated using the Eq. (23)

$$NC(w,\bar{w}) = \frac{\sum_{i=1}^{M}\sum_{j=1}^{N}[w(i,j)-\mu_w][\bar{w}(i,j)-\mu_{\bar{w}}]}{\sqrt{\sum_{i=1}^{M}\sum_{j=1}^{N}[w(i,j)-\mu_w]^2}\sqrt{\sum_{i=1}^{M}\sum_{j=1}^{N}[\bar{w}(i,j)-\mu_{\bar{w}}]^2}} \quad (23)$$

where N and M denote the number of watermark pixels. Real and extracted watermarks are w and $\bar{w}$ mean values of the extracted and genuine watermarks are represented, respectively, by $w, \bar{w}$.

We have been carried out using the MATLAB R2015a environment. And for this study, a dataset of 49 standard 512×512 grayscale test images was utilized, which was provided by the computer vision group [49]. Seven standard grayscale images, including 'Lena', 'Pepper', 'Lake', 'Zelda', 'Butterfly', 'Goldhill' and 'Baboon' with a size of 512×512, were selected as cover images, as shown in Fig. 5 from (a)–(g). A watermark image 'Desert' with a size of 512×512, as presented in Fig. 5(h), was used as the watermark. Despite the fact that just seven test images were displayed, the suggested technique was also used on additional typical test images that were taken from the aforementioned image library. The utilization of Particle Swarm Optimization (PSO) has eliminated the laborious manual process of setting various values for the scaling factor alpha and determining the optimal value from the tested range. With PSO, the scaling factor alpha is automatically selected, enabling our watermarking algorithm to attain optimal performance while maintaining a superior balance between imperceptibility and robustness. The results of watermark embedding and extraction processes for the respective images, as depicted in Fig. 5, are presented in Fig. 6.

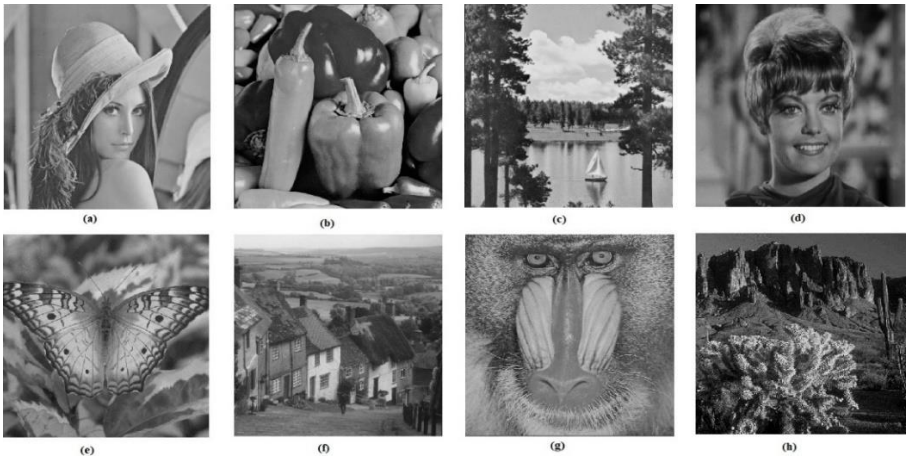

Figure 5. Input Host images for performing experiment (a) Lena (b) Pepper (c) Lake (d) Zelda (e) Butterfly (f) Goldhill (g) Baboon and watermark image (h) Desert.

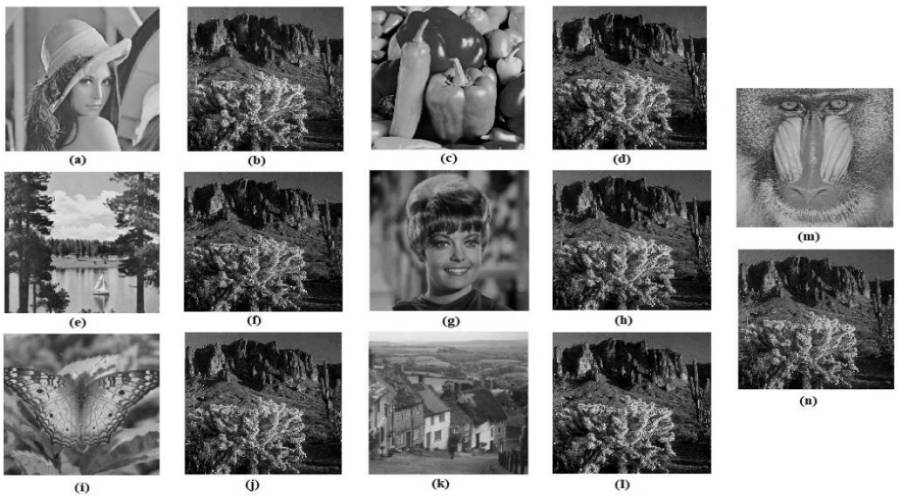

Figure 6. Test watermarked images are (a, c, e, g, I, k, m) and extracted watermark images from their respected watermarked images are (b, d, f, h, j, l, n).

A. Imperceptibility and Robustness Analysis

This subsection offers an exhaustive analysis of our proposed scheme, examining imperceptibility and robustness under the absence of attacks. Generally, a PSNR value of ≥50 dB indicates excellent image quality with no noticeable changes, while a PSNR number between 35 dB and 48 dB denotes excellent image quality, one between 29 dB and 35 dB denotes passable image quality. If the PSNR is less than 25 dB, the picture is discernible. Similarly, a high NCC (Normalized Cross-Correlation) value indicates a strong correlation between two images. In the case of our proposed scheme, we have achieved significant levels of imperceptibility and robustness. The following tables

display the values of PSNR and NCC metrics for the watermarked image and extracted watermark.

TABLE I. PSNR(DB) AND NCC VALUES BETWEEN HOST IMAGES AND WATERMARKED IMAGES UNDER NO ATTACK

Cover Image	PSNR	NCC
Lena	48.3387	1
Pepper	49.3231	1
Lake	49.9942	1
Zelda	49.3387	1
Butterfly	49.2561	1
Goldhill	49.1132	1
Baboon	49.2334	1
Average PSNR and NCC Values	**49.2282**	**1**

The analysis of the results presented in Table I showcases the exceptional imperceptibility of our proposed watermarking method. The average PSNR value of 49.2282 dB indicates high quality, while all watermarked images achieved PSNR values exceeding 45 dB. Remarkably, the 'Lake' image demonstrated the highest PSNR and NCC values, scoring 49.9942 dB and 1.0000, respectively.

Similarly, Table II presents the numerical results obtained for the original and extracted watermark. The table reveals a maximum NCC value that is extremely close to 1, indicating a remarkable level of accuracy in reconstructing the extracted watermark images. Furthermore, the PSNR values provide validation for the output. In summary, the extraction process successfully obtained the original grayscale watermark image without any noticeable distortion.

TABLE II. PSNR(DB) AND NCC VALUES BETWEEN ORIGINAL WATERMARK AND EXTRACTED WATERMARK UNDER NO ATTACK

Cover Image	PSNR	NCC
Lena	34.1873	0.9966
Pepper	33.6872	0.9961
Lake	29.3159	0.9980
Zelda	38.2141	0.9990
Butterfly	35.7086	0.9980
Goldhill	34.0699	0.9973
Baboon	36.2266	0.9980

B.. Comparative Analysis

In this section, we present a detailed comparative analysis of our proposed scheme with respect to several previously proposed schemes. To facilitate a thorough examination, this section is further divided into two sub-sections. The first sub-section focuses on a comparative analysis under normal conditions i.e., without any attacks. The second sub-section explores the performance of the watermarked image when subjected to various types of attacks, allowing for a robust evaluation of our scheme's effectiveness.

1) Analysis without attack condition

Table III presents a comparison between the watermarked image, the watermark that was retrieved using our suggested technique, and many standard techniques. It is worth noting that all methods utilized the 'Lena' image as a common test image. Upon examining the data presented in this table, it is evident that our proposed scheme surpasses the performance of the given baseline approaches in terms of imperceptibility. However, it is important to note that the NCC value of the extracted watermark using our proposed scheme is comparatively lower than that of the listed approaches. This can be attributed to the trade-off between imperceptibility, robustness, and capacity, which requires careful consideration.

TABLE III. COMPARISON OF PSNR AND NCC VALUES BETWEEN PREVIOUS SCHEMES AND PROPOSED SCHEME TAKING 'LENA' AS A HOST IMAGE, UNDER NO ATTACK

Schemes	Watermarked Image (PSNR)	Extracted watermark (NCC)
Agoyi *et al.* [31]	29.49	1
Verma *et al.* [50]	41.5107	1
Wang and Zhao [32]	40.74	1
Wang [51]	42.38	1
Das *et al.* [33]	41.78	1
Radha *et al.* [38]	62.8871	0.99125
Proposed Method	48.3387	**0.9966**

Likewise, Table IV illustrates a comparison between the watermarked image and the extracted watermark for our proposed method and several baseline approaches, all utilizing the 'Pepper' image as a standardized test image.

TABLE IV. COMPARISON OF PSNR AND NCC VALUES BETWEEN PREVIOUS SCHEMES AND PROPOSED SCHEME TAKING 'PEPPER' AS A HOST IMAGE, UNDER NO ATTACK

Schemes	Watermarked Image (PSNR)	Extracted watermark (NCC)
Agoyi *et al.* [31]	34.3	1
Verma *et al.* [50]	38.19	1
Wang and Zhao [32]	40.10	1
Hu *et al.* [30]	45.128	1
Kang *et al.* [29]	42.25	1
Radha *et al.* [38]	55.8646	0.99530
Proposed Method	49.3231	**0.9961**

Similar findings can be observed from this table, highlighting the superior performance of our proposed scheme compared to all the listed schemes in a no-attack scenario. In summary, based on the results presented in Tables III and IV, along with the accompanying discussion, it is evident that our proposed algorithm achieves excellent transparency for both the watermarked image and the extracted watermark in the absence of any attacks.

2) Analysis with attacks condition

To assess the resilience of our proposed scheme against attacks, we conducted a series of experiments where the watermarked image was subjected to various types of attacks. These attacks included Gaussian noise, histogram equalization, speckle noise, salt and pepper noise, median filter, average filter, Gaussian filter, resizing, cropping, and rotation. The results of the aforementioned experiment are displayed in Table V.

The distorted watermarked images subjected to the above mentioned attacks are shown in the Fig. 7. Table V provides detailed performance data for the proposed scheme. The performance evaluation involves calculating the Peak Signal-to-Noise Ratio (PSNR) between the watermarked image after the attack and the original cover image, as well as the Normalized Cross-Correlation (NCC) between the extracted watermark from the attacked watermarked image and the original watermark. Analysing the table reveals that our proposed scheme exhibits significant robustness, particularly against rotation and cropping attacks. The NCC values for each attack surpass 0.9500, providing strong evidence of the scheme's resilience. Notably, when the watermarked images are subjected to a 25% cropping, they experience substantial distortion as indicated by the PSNR mean value falling below 13 dB. With a medium NCC, the retrieved watermarks are still clearly visible. value exceeding 0.9900. This high NCC value demonstrates that the system is highly reliable and can effectively resist attempts to compromise the integrity of the watermarked images, even when faced with deliberate attacks.

TABLE V. PSNR AND NCC VALUES AFTER APPLYING DIFFERENT ATTACKS ON THE AFOREMENTIONED COVER IMAGES

Schemes	**Images**													
	Lena		**Pepper**		**Lake**		**Zelda**		**Butterfly**		**Goldhill**		**Baboon**	
	PSNR	**NCC**	**PSNR**	**NCC**	**PSNR**	**NCC**	**PSNR**	**NCC**	**PSNR**	**NCC**	**PSNR**	**NCC**	**PSNR**	**NCC**
Gaussian Noise (0.01)	20.0519	0.9993	20.2505	0.9994	20.1543	0.9993	20.1868	0.9994	20.0358	0.9995	20.1083	0.9995	20.0336	0.9985
Histogram Equalization	19.2712	0.9865	18.6193	0.9851	23.8810	0.9871	18.1495	0.9850	17.2847	0.9888	17.5459	0.9879	18.2445	0.9973
Speckle Noise (0.05)	20.1829	0.9971	19.7515	0.9994	18.6300	0.9990	21.1643	0.9998	19.3004	0.9994	19.7686	0.9997	18.7079	0.9991
Salt & Pepper Noise (0.05)	18.6126	0.9977	18.1207	0.9974	18.0552	0.9977	18.2683	0.9968	18.5237	0.9987	18.3302	0.9978	19.6466	0.9993
Median Filter (3×3)	35.2403	0.9769	32.1766	0.9925	27.1763	0.9721	34.3779	0.9770	28.3566	0.9723	28.8302	0.9739	22.6351	0.9594
Average Filter (3×3)	32.3512	0.9754	31.5930	0.9725	29.6477	0.9704	35.1450	0.9763	29.8078	0.9697	29.7982	0.9727	24.5453	0.9593
Gaussian Filter (3×3)	43.2337	0.9954	40.5715	0.9759	38.3358	0.9749	43.2912	0.9780	38.6559	0.9744	39.8144	0.9764	33.1488	0.9700
Resizing (512-256-512)	34.3789	0.9981	32.0752	0.9992	30.3129	0.9971	35.3582	0.9897	29.6829	0.9973	31.3233	0.9972	25.3247	0.9980
Cropping (25%)	13.7912	0.9978	11.1218	0.9917	10.7283	0.9963	12.1323	0.9997	11.2384	0.9993	11.8759	0.9981	11.4928	0.9998
Rotation (45^{o})	11.5421	0.9981	10.1528	0.9935	9.2879	0.9982	11.0532	0.9973	10.1432	0.9887	10.5153	0.9789	10.1413	0.9898

Figure 7. Noisy Watermarked images (a0–a9)) Lena (b0–b9) Pepper (c0–c9) Lake (d0–d9) Zelda (e0–e9) Butterfly (f0–f9) Goldhill (g0–g9) Baboon after applying Ten different attacks.

A comparative analysis of the NCC values of the extracted watermark between our proposed method and several baseline approaches has also been performed. The results of this analysis are presented as follows:

On the basis of the data presented in Tables VI and VII, it becomes apparent that our proposed scheme exhibits superior performance compared to the listed approaches in terms of robustness. This affirms the strength of our proposed scheme even in the presence of external threats. Overall, our scheme excels in terms of both imperceptibility and robustness.

TABLE VI: COMPARISON OF NCC VALUES OF EXTRACTED WATERMARK BETWEEN PREVIOUSLY PRESENTED SCHEME AND PROPOSED SCHEME, TAKING 'LENA' AS HOST IMAGE

Attacks	Kang *et al.* [29]	Hu *et al.* [30]	Agoyi *et al.* [31]	Wang and Zhao [32]	Radha *et al.* [38]	Proposed Method
Gaussian Noise (0.01)	0.8142	0.939 (0.005)	0.6362	0.9983 (0.001)	0.90314 (0.002)	0.9993
Histogram Equalization	0.9953	0.962	0.9776	0.8176	0.90352	0.9865
Speckle Noise (0.05)	0.8075	0.980 (0.005)	-	0.9955 (0.01)	0.90607	0.9971
Salt & Pepper Noise (0.05)	0.8386 (0.02)	0.983	-	0.9868 (0.01)	0.9443	0.9977
Median Filter (3×3)	0.9967	0.956	-	0.9971	-	0.9769
Average Filter (3×3)	0.9641	-	-	-	0.90613	0.9754
Gaussian Filter (3×3)	1.0000	-	-	0.9959	-	0.9778
Resizing (512-256-512)	0.9987	0.6408	−0.6178	0.9977	0.90680	0.9992
Cropping (25%)	0.9574	-	-	-	-	0.9978
Rotation (45°)	-	-	-	0.3928	0.92069	0.9981

TABLE VII. COMPARISON OF NCC VALUES OF EXTRACTED WATERMARK BETWEEN PREVIOUSLY PRESENTED SCHEME AND PROPOSED SCHEME, TAKING 'PEPPER' AS HOST IMAGE

Attacks	Kang *et al.* [29]	Hu *et al.* [30]	Agoyi *et al.* [31]	Want and Zhao [32]	Radha *et al.* [38]	Proposed Method
Gaussian Noise (0.01)	0.8052	0.904 (0.005)	0.6684	0.9986 (0.001)	0.91885 (0.002)	0.9994
Histogram Equalization	0.9960	-	0.8968	0.8579	0.98002	0.9851
Speckle Noise (0.05)	0.8166	0.995 (0.005)	-	0.9964 (0.01)	0.97484	0.9994
Salt & Pepper Noise (0.05)	0.8544 (0.02)	0.982	-	0.9782 (0.01)	0.98770	0.9974
Median Filter (3×3)	0.9765	-	-	0.998	-	0.9748
Average Filter (3×3)	0.9641	-	-	-	0.98994	0.9725
Gaussian Filter (3×3)	1.0000	-	-	0.9955	-	0.9759
Resizing (512-256-512)	0.9987	-	−0.5948	0.9942	0.73432	0.9981
Cropping (25%)	0.9588	-	-	-	-	0.9917
Rotation (45°)	-	-	-	0.1365	0.97427	0.9935

V. CONCLUSION

This paper presents a hybrid DWT-SVD-based adaptive image watermarking scheme. In this scheme, one-level DWT is used to decompose the original host image and the watermark, and subsequently, SVD is applied on the LL sub-band of both the decomposed images. Later on, the eigenvalues of the original input image are modified by the eigenvalues of the watermark. And then, inverse SVD and inverse DWT are applied to get the watermarked image. To get the extracted watermark, the inverse of the embedding process is applied. The presented scheme aims to combine the strengths of DWT and SVD in order to increase the effectiveness of watermarking. Specifically, DWT provides advantages such as spatial and frequency localization, while SVD improves the watermark's resilience against various types of attacks. Thus, the combination of both schemes improves the imperceptibility and robustness of the watermarking scheme. The scaling factor plays an important role in determining the embedding strength, and choosing the scaling factor is a tedious task to strike a balance between imperceptibility, robustness, and capacity. In this scheme, an optimization method called particle swarm optimization is utilized for determining the scaling factor. The utilization of PSO makes the presented watermarking scheme adaptive. Although the utilization of optimization method increases the complexity of the watermarking scheme, this reduces the overall time complexity of the process since the task of finding an optimal scaling factor is now handled by the optimization method. On the basis of the experimental results and analysis presented in this paper, it is clearly established that the presented scheme is overall superior in terms of imperceptibility, robustness, and capacity with respect to previously presented schemes. The limitations of our presented scheme are that it is designed for grayscale images and is not reliable for binary images, which limits its future scope. Secondly, we can also make this scheme suitable for multi-image watermarking.

CONFLICT OF INTEREST

The authors declare no conflict of interest.

AUTHOR CONTRIBUTIONS

Sachin Gaur conducted the research, analysed the data, proposed the methodology, and wrote the initial draft; Navneet Tripathi check the experiment of the research and

modified the initial draft; Jyoti Pandey has written the final version of the manuscript. All authors had approved the final version.

ACKNOWLEDGMENT

The authors of this article would like to thank all participants who provided data for this work.

REFERENCES

[1] C. I. Podilchuk and E. J. Delp, "Digital watermarking: Algorithms and applications," *IEEE Signal Process. Mag.*, vol. 18, no. 4, pp. 33–46, 2001.
[2] P. Taylor, V. S. Verma, and R. K. Jha, "An overview of robust digital image watermarking an overview of robust digital image watermarking," *IETE Tech. Rev.*, vol. 11, no. 4, pp. 37–41, 2015.
[3] N. Tarhouni, M. Charfeddine, and C. Ben, "Novel and robust image watermarking for copyright protection and integrity control," *Circuits, Syst. Signal Process.*, vol. 39, 2020.
[4] L. Zhang, J. W. Xiao, and J. Y. Luo, "A robust color image watermarking based on SVD and DWT," *Int. J. Communication*, vol. 3, pp. 62–65, 2014.
[5] A. Ray and S. Roy, "Recent trends in image watermarking techniques for copyright protection : A survey," *Int. J. Multimedia. Inf. Retr.*, vol. 9, 2020.
[6] G. Coatrieux, L. Lecornu, and B. Sankur, "A review of image watermarking applications in healthcare," in *Proc. Conf. IEEE Eng Med Biol Soc*, 2006, pp. 4691–4694.
[7] N. Nikolaidis and I. Pitas, "Robust image watermarking in the spatial domain," *Signal Processing*, vol. 66, no. 3, pp. 385–403, 1998.
[8] A. K. Sahu and G. Swain, "An optimal information hiding approach based on pixel value differencing and modulus function," *Wireless Pers. Communication*, vol. 21, no. 7, pp. 1–16, 2019.
[9] A. Bamatraf and R. Ibrahim, "Digital watermarking algorithm using LSB," in *Proc. International Conference on Computer Applications and Industrial Electronics (ICCAIE 2010)*, 2010, pp. 155–159.
[10] M. Hussain *et al.*, "Image steganography in spatial domain: A survey," *Signal Process. Image Communication*, vol. 65, pp. 46–66, 2018.
[11] W. N. Cheung, "Digital image watermarking in spatiand transform domains," in *Proc. TENCON*, Kuala Lumpur, Malaysia, 2000, pp. 374–378.
[12] C. Pun, "A novel DFT-based digital watermarking system for images," in *Proc. ICSP 2006*, 2006, vol. 2, no. 8, pp. 3–6.
[13] T. K. Tewari, "An improved and robust DCT based digital image watermarking scheme," *Int. J. Computer. Appl.*, vol. 3, no. May 2014, pp. 28–32, 2010.
[14] G. Tianming and W. Yanjie, "DWT-based digital image watermarking algorithm," in *Proc. IEEE 2011 10th International Conference on Electronic Measurement & Instruments*, 2011, no. 2, pp. 163–166.
[15] B. L. Gunjal, "An overview of transform domain robust digital image watermarking algorithms," *J. Emerge Trends Computer. Inf. Sci.*, vol. 2, no. 1, pp. 37–42, 2010.
[16] K. Deb, S. Al-seraj, M. Hoque, and I. H. Sarkar, "Combined DWT-DCT based digital image watermarking technique for copyright protection," in *Proc. 7th Int. Conf. Electr. Computer. Eng.*, 20-22 December, Dhaka, Bangladesh, 2012, pp. 458–461.
[17] A. K. Sahu and G. Swain, "An improved data hiding technique using bit differencing and LSB matching," *Internetworking Indones. J.*, vol. 10, no. January 2018, pp. 17–21, 2019.
[18] V. S. Rao, S. R. Shekhawat *et al.*, "A DWT-DCT-SVD based digital image watermarking scheme using particle swarm optimization," in *Proc. IEEE Students' Conf. Electr. Electron. Computer. Sci.*, 2012, pp. 10–13.
[19] S. D. Lin, S. Shie, and J. Y. Guo, "Improving the robustness of DCT-based image watermarking against JPEG compression," *Computer. Stand. Interfaces*, vol. 32, no. 1–2, pp. 54–60, 2010.
[20] F. Yasmeen and M. S. Uddin, "An efficient watermarking approach based on LL and HH edges of DWT-SVD," *SN Computer. Sci.*, vol. 2, no. 2, pp. 1–16, 2021.
[21] T. Thakkar and V. K. Srivastava, "A particle swarm optimization and block-SVD-based watermarking for digital images," *Turkish J. Electr. Eng. Computer. Sci.*, vol. 25, no. 8, pp. 3273–3288, 2017.
[22] A. Zear, A. K. Singh, and P. Kumar, "A proposed secure multiple watermarking technique based on DWT, DCT and SVD for application in medicine," *Multimedia. Tools Appl.*, vol. 77, no. 8, pp. 1–20, 2016.
[23] V. Kumar, R. Lautan, M. Faisal, and K. M. Pandey, "DWT and particle swarm optimization based digital image watermarking," *Int. J. Eng. Res. Technol.*, vol. 2, no. 9, pp. 2144–2149, 2013.
[24] Y. Liu, S. Tang, R. Liu, L. Zhang, and Z. Ma, "Secure and robust digital image watermarking scheme using logistic and RSA encryption yang," *Expert Syst. Appl.*, vol. 97, pp. 95–105, 2017.
[25] N. Wu and M. Hwang, "A novel LSB data hiding scheme with the lowest distortion," *Imaging Sci. J.*, vol. 65, no. 9, pp. 1–8, 2017.
[26] K. T. K. Kuppusamy, "Optimized image watermarking scheme based on PSO," in *Proc. Int. Conference Model. Optim. Computer.*, 2012, vol. 38, pp. 493–503.
[27] A. Gorai, "Gray-level image enhancement by particle swarm optimization," in *Proc. IEEE Int. Conf. Computer. Intell Communication. Technol.*, 2009, no. 1, pp. 72–77,
[28] R. A. Ghazy, N. A. El-fishawy, M. M. Hadhoud, M. I. Dessouky, and F. E. A. El-Samie, "An efficient block-by-block SVD-based image watermarking scheme," in *Proc. IEEE Conference Natl. Radio Sci.*, 2007, pp. 1–9.
[29] X. Kang, Y. Chen, F. Zhao, and G. Lin, "A novel hybrid of DCT and SVD in DWT domain for robust and invisible blind image watermarking with optimal embedding strength," *Multimedia Tools Application*, vol. 77, no. 11, pp. 1–28, 2017.
[30] K. Hu *et al.*, "Robust and efficient image watermarking via EMD and dimensionality reduction," *Visual Computer.*, 2021.
[31] M. Agoyi, E. Çelebi, and G. Anbarjafari, "A watermarking algorithm based on chirp z-transform, discrete wavelet transforms and singular value decomposition," *Signal Image and Video Processing*, February 2014.
[32] B. Wang and P. Zhao, "An adaptive image watermarking method combining SVD and Wang-Landau sampling in DWT domain," *Math. Artic.*, vol. 8, pp. 1–21, 2020.
[33] C. Das, S. Panigrahi, V. K. Sharma, and K. K. Mahapatra, "A novel blind robust image watermarking in DCT domain using inter-block coefficient correlation," *AEUE - Int. J. Electron. Communication*, vol. 68, no. 7, pp. 1–10, 2013.
[34] N. M. Makbol, B. E. Khoo, T. H. Rassem, and K. Loukhaoukha, "A new reliable optimized image watermarking scheme based on the integer wavelet transform and singular value decomposition for copyright protection," *Inf. Sci. (Ny).*, vol. 417, no. 37, pp. 381–400, 2017.
[35] S. Roy and A. K. Pal, "A robust blind hybrid image watermarking scheme in RDWT-DCT domain using Arnold scrambling," *Multimedia Tools Appl.*, 2016.
[36] M. Ali, C. W. Ahn, M. Pant, and P. Siarry, "A Reliable image watermarking scheme based on redistributed image normalization and SVD," *Discrete. Dyn. Nat. Soc.*, vol. 5, no. 8, pp. 1–15, 2016.
[37] I. A. Ansari and M. Pant, "Multipurpose image watermarking in the domain of DWT based on SVD and ABC," *Pattern Recognition. Lett.*, vol. 94, pp. 1–12, 2016.
[38] R. R. Kumaria, V. V. Kumar, and K. R. Naidu "Deep learning-based image watermarking technique with hybrid DWT-SVD," *The Imaging Science Journal*, vol. 51 pp. 1–18, 20 June 2023. doi:10.1080/13682199.2023.2223080
[39] A. Al-Ha, "Combined DWT-DCT digital image watermarking," *J. Computer. Sci.*, vol. 3, no. 9, pp. 740–746, 2007.
[40] M. Hsieh, D. Tseng, and Y. Huang, "Hiding digital watermarks using multiresolution," *IEEE Transactions on Industrial Electronics*, vol. 48, no. 5, pp. 875–882, 2001.
[41] C. Hsu and J. Wu, "Multiresolution watermarking for digital images," *IEEE Trans. CIRCUITS Syst.*, vol. 45, no. 8, pp. 1097–1101, 1998.
[42] A. Nikolaidis, I. Pitas, and S. Member, "Asymptotically optimal detection for additive watermarking in the DCT and DWT domains," *IEEE Transactions on Image Processing*, vol. 12, no. 5, pp. 563–571, 2003.
[43] W. C. Chu, "DCT-based image watermarking using subsampling," *IEEE Trans. Multimedia*, vol. 5, no. 1, pp. 34–38, 2003.

[44] S. M. Arora, "A DWT-SVD based robust digital watermarking for digital images," *Procedia Computer. Sci., Science Direct*, vol. 132, pp. 1441–1448, 2018.
[45] P. Bao and X. Ma, "Transactions Letters, image adaptive watermarking using wavelet domain singular value decomposition," *IEEE Trans. Circuits Syst. Video Technol.*, vol. 15, no. 1, pp. 96–102, 2005.
[46] S. Al-mansoori and A. Kunhu, "Robust watermarking technique based on dct to protect the ownership of dubaisat-1 images against attacks," *Int. J. Computer Science Network Security*, vol. 12, no. June, pp. 1–9, 2012.
[47] M. A. Mohamed and A. M. El-mohandes, "Hybrid DCT-DWT watermarking and idea encryption of internet contents," *Int. J. Computer. Science*, vol. 9, no. 1, pp. 394–401, 2012.
[48] E. E. Hemdan, N. El-fishawy, G. Attiya, and F. E. A. El-Samie, "An efficient image watermarking approach based on wavelet fusion and singular value decomposition in wavelet domain," in *Proc. 3rd Int. Conference. Adv. Control Circuit Syst.*, vol. 1–10, no. May 2016.
[49] Computer vision group. Dataset of standard 512×512 grayscale test images. [Online]. Available: https://ccia.ugr.es/cvg/CG/base.htm
[50] V. S. Verma, R. K. Jha, and A. Ojha, "Digital watermark extraction using support vector machine with principal component analysis based feature reduction," *J. Vis. Commun. Image Represent*, vol. 31, pp. 75–85, 2015.
[51] T. Wang, "Digital image watermarking using dual-scrambling and singular value decomposition," in *Proc. 2017 IEEE International Conference on Computational Science and Engineering (CSE) and IEEE International Conference on Embedded and Ubiquitous Computing (EUC)*, IEEE, 2017, vol. 1, pp. 724–727.